energies

MDPI

Article

Operating Lifetime Behavior of Thermal Contact Resistance Between Clip-Attached TO 247 Package and Heat Sink with and Without an Ultra-Thin Interlayer Silver Film

Zsolt Toth-Pal * **and Hans-Peter Nee**

EECS, KTH Royal Institute of Technology, SE 10044 Stockholm, Sweden; hansi@kth.se
* Correspondence: zsolttp@kth.se; Tel.: +46-706257182

Abstract

The thermal contact resistance between a clip-attached TO 247 package and heat sink is a very large contributor to the total thermal resistance. Therefore, it is important to investigate its reliability and lifetime behavior. The novelty of this investigation is the new, detailed lifetime behavior measurement results of thermal contact resistance between package and heat sink. We have carried out an accelerated lifetime test on 30 samples at 110 °C with acceleration factor of 35 for 18 weeks, corresponding to 12.1 years operating life in indoor environments. The samples were 7 without interlayer film, 12 with 12.5 µm thick silver film and 11 with 6 µm thick silver film. At the start of the test, the average of the thermal contact resistance of samples with 12.5 µm silver film was 20.7% lower, and with 6 µm silver film, the average of thermal contact resistance was 8.7% lower than the average of thermal contact resistance of samples without film. During the first operating month, thermal contact resistance decreased by an average of 5%. Then followed an additional 5% decrease for 12 years. All individual samples show lower thermal contact resistance after 12.1 years compared to the start. No failures were observed, not even among high outliers. By a visual inspection of heat sink surfaces, high outliers can be avoided from start. The thermal contact resistance variation is smaller for samples with silver films compared to samples without film. Samples show decreasing thermal contact resistance with increasing dissipated power. Several previously known stabilizing mechanisms can hypothetically explain the results. Not only the softness of silver, but also the high ductility and Poisson Ratio, which elongate a 12.5 µm thick film more than a 6 µm thick µm film, are hypothesized to better fill out microscopic voids. We observe silver film surface structure changes when comparing aged silver films to un-aged silver films, indicating material movements, but no exact mechanism could be proven. Therefore, the explanations studied are hypothetical. Since all measured thermal contact resistances were lower after 12.1 years, our conclusion is that stabilizing types of mechanisms are dominant during the operating lifetime for indoor environments.

Keywords: thermal contact resistance; electronics cooling; component; power package; TO 247; thermal interface material; accelerated lifetime testing; reliability; silver; thin films

Check for updates

Academic Editor: Vincenzo d'Alessandro

Received: 18 June 2026
Revised: 16 July 2026
Accepted: 22 July 2026
Published: 24 July 2026

1. Introduction

Power electronics has gone through a very significant evolution in power handling capabilities in the last decade, with the introduction of SiC power devices, resulting in increased integration of components and diminishing size of power systems and subsystems. At increased power densities in power electronic systems, a more concentrated heat generation is anticipated.

Parallel to the increased and concentrated heat generation from power chips, new, more advanced cooling techniques have been developed for power electronics [1]. Employment of active cooling techniques, such as heat pipes and usage of two-phase materials as coolants and development of jet impingement techniques, has resulted in significantly improved cooling capabilities [2,3]. Simulation-based optimization of passive cooling devices, such as heat sinks, has also significantly contributed to more efficient cooling [4].

There are three major thermal interfaces constituting the largest obstacles for efficient cooling in a typical electronic subsystem. The first is inside the package between the chip and the package heat spreader. The second, and often largest obstacle, is the thermal interface between the package and the heat sink, and the third interface is between the heat sink and the environment. If there are no thermal interface materials, nor advanced cooling methods employed, in the interface, two materials touch each other with their surface roughness and planarity issues resulting in microscopic voids at the interface, filled with air, which makes it a significant obstacle for heat conduction. A large contribution to the total thermal resistance between the power semiconductor device junction to ambient comes from the thermal contact resistance between the power package and heat sink. One additional difficulty in optimizing the thermal interface between the package and heat sink is that these parts come very often from different manufacturers with production qualities of surfaces not adjusted to each other. The reliability of power packages and their thermal effects on junction temperature and lifetime have been widely studied [5–7], but the reliability and lifetime behavior of the relatively large thermal contact resistance between the package and heat sink is less investigated. Therefore, the operating lifetime behavior of thermal contact resistance between the package and heat sink is of importance in understanding the general reliability of power subsystems.

One of the most used package types for discrete power components is the TO 247 power package. There is a large variety of attachment methods of the TO 247 packages to heat dissipating surfaces. Most widely used are clips and screw attachments. Clip attachment generates the lowest mechanical pressure between the TO 247 package and the heat sink and therefore results in higher thermal contact resistances compared to other attachment methods. If we can demonstrate improvements of thermal contact resistance at the low pressures of clip attachment, at least similar improvements can be expected at higher attachment pressures. An investigation of the reliability and lifetime behavior of the clip attachment's thermal interface resistance is therefore a priority.

Optimization of complex thermal interface materials is a difficult task [8,9] and therefore an analysis of simple metallic materials is of importance. Silver is widely used in microelectronics and packaging as conductive interconnect and interlayer material and in adhesives [10,11]. Gold is also a soft material with a low oxidation rate; however, the cost of ultra-thin gold films at the same thickness is more than three times that of silver films. This makes gold films difficult to widely introduce as interlayer material. Ultra-thin silver films with thicknesses of 2 μm–20 μm are less studied but of interest as interlayer material between the package and heat sink because the silver film's possible ability to fill out microscopic voids.

This study aims to answer two research questions: How does the thermal interface resistance between the TO 247 package and aluminum heat sink behave during operating lifetime? What improvements can we obtain by introducing an ultra-thin silver film as a thermal interface layer? The aim of our investigation was to achieve quantitative measurement results over the behavior of the thermal contact resistance between a clip-

https://doi.org/10.3390/en19153493

attached TO 247 package and heat sink over its lifetime, in an indoors, static environment, which represents the basis of further reliability analysis in different environments.

2. Materials and Methods

2.1. Method for Measuring Thermal Contact Resistance

The mechanical pressure from a commercial clip towards a TO 247 power package and heat sink is in the order of 0.1–0.6 MPa and represents the lowest pressure on average among different mechanical attachment methods. Since thermal contact resistance rapidly increases with decreasing mechanical pressure [12,13], it is important to investigate possible improvement methods of thermal contact resistance, especially when using commercial clips, and monitor also the thermal contact behavior during the operating lifetime.

The concept of our measurement method of thermal contact resistance between a TO 247 package and aluminum heat sink is shown on Figure 1. From the heat generating power diode inside the TO 247 package, the heat flow was directed towards the fins of the heat sink by immersing it into ice water. Thermal sensors of type Pt 1000 were attached to the heat sink and the TO 247 package, respectively. The thermal contact resistance between the package and heat sink was measured by dividing the temperature difference measured between the package and the heat sink by the measured dissipated power of the power diode.

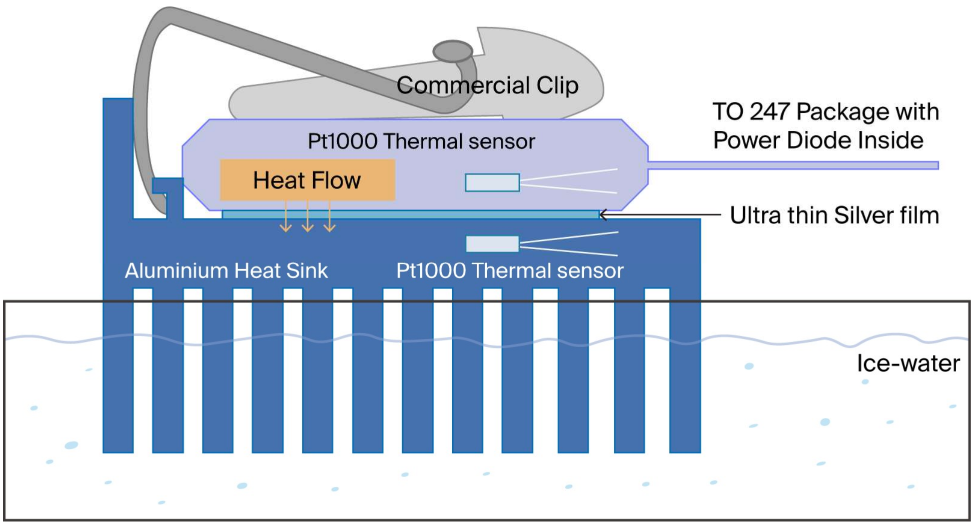

Figure 1. The concept of the heat transfer experiment.

2.2. Experiment Design

We designed our experiment to minimize the thermal interaction between the top side of the heat sink and the surrounding air and direct the heat flow down towards the ice water at 0 °C. We chose a heat sink with thermal resistance of 1 K/W resulting in the temperature of the top side of the heat sink to be around 22 °C, close to the surrounding air temperature, when 22 W of power was dissipated on average from the power diode [14].

The Pt 1000 type of thermal sensor was chosen, with 1000 Ohm resistance at 0 °C, to minimize the influence of parasitic electrical contacting resistances.

The Pt 1000 sensor attached to the TO 247 package was placed as close as possible to the thermal interface of the package. It was attached by thermal glue in the corner on the side of the TO 247 package where the sensor also had contact with the heat spreader metal of the TO 247 package. The distance to the interface was not more than 3–4 mm. However, this placement of the sensor resulted in a lower temperature measured compared to the true temperature of the thermal interface on the package side. The difference can be described as the parasitic heat flow from the package towards the Pt 1000 sensor, times the thermal spreading resistance of the metal heat spreader over the 3–4 mm distance.

The Pt 1000 sensor attached to the heat sink was placed also as close as possible to the heat sink side of the thermal interface on the side of the package with the thermal glue at a distance also of 3–4 mm from the interface. Closer placement was not possible because of the risk of the thermal glue getting in thermal contact with the TO 247 package by accident. This placement of the sensor resulted also in a lower temperature measured compared to the true temperature of the thermal interface on the heatsink side. The difference can be described also here as the parasitic lateral heat flow from the heat sink interface to the Pt 1000 sensor, times the heat sink lateral thermal spreading resistance over 3–4 mm.

The resulting difference, or temperature difference measurement error, due to the placements of sensors, is only the difference between these two above-described measurement differences. Since the placement distances are similar, the heat flows are through metals with low heat resistivities (for aluminum typically 0.00422 m·K/W). By our experiment design, we had low parasitic lateral heat flows, and we did not compensate in our calculations for this error. As a verification that no major source of error was affecting the thermal contact resistance measurements, a comparison between measured and calculated thermal contact resistance was presented in [14] where the same measurement method was employed, using the calculation formula from [13]. We carried out also control measurements by placing two Pt 1000 sensors on the heat sink side and measured the temperature difference between the sensors. The difference was only 0.25 °C while the temperature difference between the heat sink and package was 31.2 °C at 22.3 W dissipated power, resulting in a shift of measured thermal contact resistance only by 0.8%.

2.3. Experiment Description

For each thermal contact resistance measurement, fresh ice water was prepared, and the fins of the aluminum heat sink were immersed in it. Before powering up the diode, the temperatures of the heat sink and the TO 247 package were monitored to cool down below 5 °C, verifying adequate thermal contacts between the package, the heat sink and the ice water. A photograph of the experimental setup is shown in Figure 2. After the silicon power diode was turned on, 18 A of current was forced through it, and the diode voltage drop was measured on the pins of the package. Around 22 W of power was dissipated. The temperature of the package and the heat sink were measured every 5 min during 15 min of thermal stabilization time. During this stabilization, we monitored also the temperature difference to remain almost constant between package and heat sink. After 15 min of thermal stabilization, we measured the temperatures at the TO 247 package and the heat sink, and we calculated the temperature difference from these simultaneous single measurements. This difference is divided by the dissipated power, resulting in the thermal contact resistance. We used this static measurement method because of its simplicity, compared to dynamic methods [15,16].

Since each clip, package and heat sink have a unique combination of clip mechanical pressure, package thickness and heat sink surface quality, each experimental sample has shown its unique thermal contact resistance.

2.4. Materials Used

The materials used in our experiments were as follows:

1. Mechanical clips designed for TO 247 packages—30 pieces.
2. TO 247 packaged Si power diodes with T junction max = 175 °C—30 pieces.
3. 6 µm and 12.5 µm thick high purity silver films—11 and 12 pieces.
4. 1 K/W thermal resistance, aluminum, degreased, finish heat sinks—30 pieces.

https://doi.org/10.3390/en19153493

5. Pt 1000 type of temperature sensors—60 pieces.
6. 5.6 mm diameter meander type of pressure (force) sensor—1 piece.

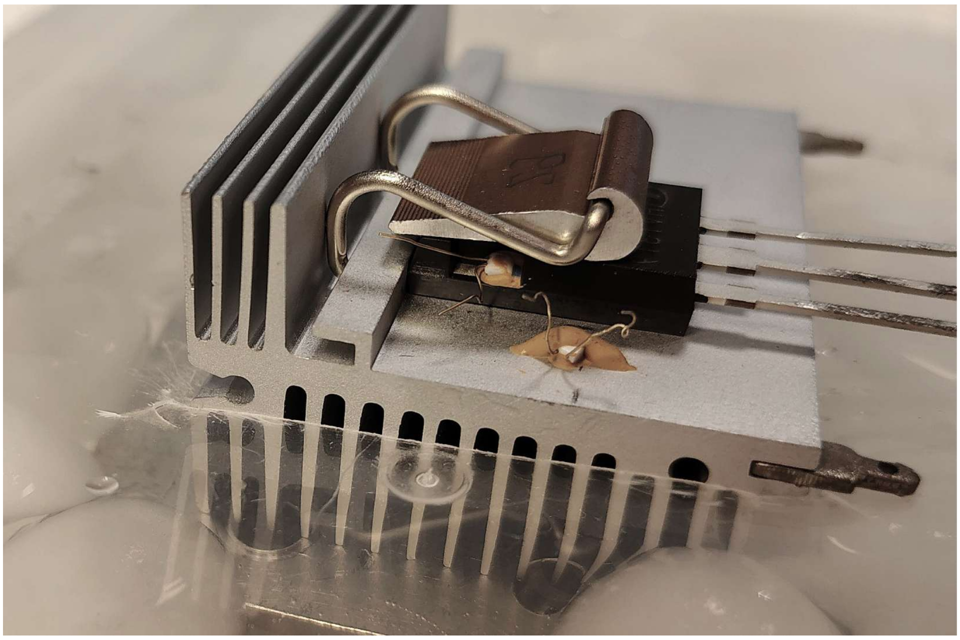

Figure 2. Photograph of the experiment setup.

2.5. Sample Preparation

The most important parameters affecting the thermal contact resistance between heat sinks and clip-attached TO 247 packages are the heat sink surface roughness and planarity, the mechanical pressure from the clip on the package, and the TO 247 package thickness. Every sample has its unique combination of these parameters; therefore, a significant number of samples had to be prepared to give a realistic picture of the distribution of thermal contact resistance, its behavior during the operating lifetime and possible failure. We prepared 30 samples [17]: 7 without any interlayer film, 12 with 12.5 µm interlayer silver film and 11 with 6 µm interlayer silver film.

Before mounting the samples, the contact surfaces of all 30 heat sinks were visually inspected and classified from the smoothest surface to the roughest surface in 7 quality classes and numbered in increasing order. The package thicknesses of all 30 TO 247 packages were measured and found to vary only by 0.012 mm from 4.998 mm to 5.010 mm. Even so, the packages were sorted in a decreasing thickness order. The mechanical pressures from all 30 clips were measured on the same reference TO 247 package and heat sink by the 5.6 mm diameter meander type of pressure sensor.

At mounting, the samples were combined with the smoothest surface paired with the thickest TO 247 package, and with the clip giving the highest pressure, resulting in an expected best combination for the thermal contact resistance. The sample mounting continued then towards the worst possible combination. A table with exact combinations of heat sink surface classification, measured package thicknesses and clip pressures, together with how these were paired to specific samples, is available in the supporting Excel data file. Samples without film and with 12.5 µm and 6 µm films were evenly distributed over the quality distribution of these 30 samples. By this method, we created the wide spread of combinations for thermal contact resistance, wider than an arbitrary combination. Figure 3 shows a visual difference between three heat sink surfaces: the smoothest heat sink surface on the left, a typical surface in the center and the roughest on the right side of the picture. At more rough heat sink surfaces, we see obvious roller marks parallel to the fins on the surface originating from the heat sink manufacturing process. The general recommendation for heat sink surface roughness is Ra = 0.4–1.6 µm. Surface roughness measurements are done in one line, giving quantitative results. The human eye can quickly and with good sensitivity scan in two dimensions and recognize patterns but does not give quantitative results. In this study, we used a visual classification resulting in 7 classes, and out of that only 1 class was recognized as outlier. The exact result of this classification is available in the supporting Excel document.

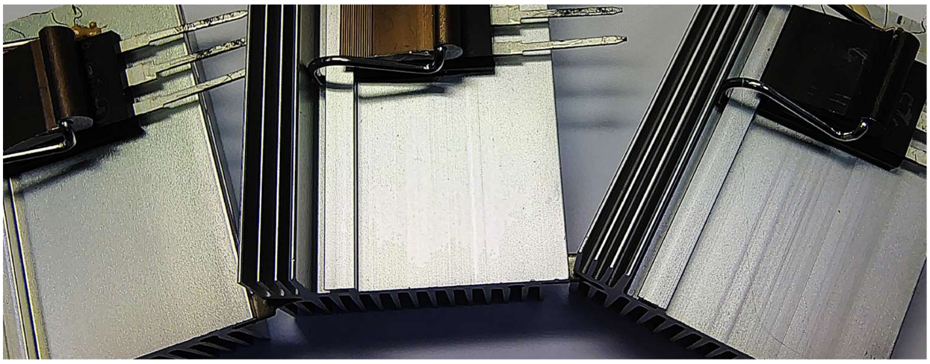

Figure 3. Photograph of 3 heatsink surfaces: with the smoothest surface on the left, a typical surface in the center and the roughest in the right of the picture.

As a clip was locked to a TO 247 package when mounting a sample, it was never opened again during the accelerated lifetime test and measurements. In this way, we ensured the undisturbed continuity of the same clip pressure along the lifetime test.

The samples were named with the following convention: A letter N denotes no film sample, S denotes a silver film sample with 12.5 µm silver film, and S with a small t (thin) at the end of the sample name denotes 6 µm silver film. After the letter comes the numbering of the sample. Samples which were regarded as outliers already before the first measurements are denoted with a big O letter in the beginning of the sample name. The two letters AG at the end of the name denote the Advance Group samples. In the middle of the sample, name there is a slash, and after the slash is the heat sink identifying number. The lower the heat sink number, the better the heat sink surface quality. Some samples have a heat sink identifier starting with D, meaning the sample is from one separately purchased batch.

2.6. Method for Monitoring Operating Lifetime

For evaluation of operating lifetime behavior of thermal contact resistance, we carried out an accelerated high temperature storage test. The maximum operating temperature of the Si power devices with the TO247 packages and heat sinks with clips were specified above 120 °C. However, the maximum operating temperature of the thermal glue for the Pt 1000 sensors' attachments was specified to 120 °C. For this reason, we set the oven temperature for the accelerated operating life test to 110 °C.

Since the package-to-heat-sink interface temperature for all different industrial applications is not possible to know, we have to accept the generally used average temperature of 55 °C as the average thermal interface temperature during the operating lifetime [18]. With this input data, we obtained an acceleration factor of 35, as described in detail in Section 2.7. For applications with other, especially higher interface, temperatures, an adjustment of the acceleration factor must be made. Figure 4 shows the experiment samples placed in the test oven.

Figure 4. The experiment samples were placed in oven for accelerated lifetime test.

The thermal contact resistances of all samples were measured at the start of the test and after 12 h, 24 h, 48 h, 1 week, 2 weeks, 4 weeks, 6 weeks, 8 weeks, 10 weeks, 12 weeks, 14 weeks, 16 weeks, and 18 weeks in the test. All samples were simultaneously put into and taken out from the oven and all samples were allowed to naturally cool down to room temperature before measurements started.

The dependence on dissipated power of the thermal contact resistance was measured for 3 samples (1 with 12.5 µm silver film, 1 with 6 µm silver film and 1 without film) at start and after 6, 12, and 18 weeks in the test. At measurements, on a few occasions, new Pt1000 sensors with new thermal glue were attached and the temperature was measured both with the new sensors and the sensors submitted to oven treatment. No significant differences were observed, proving that level of aging of the thermal glue and the thermal sensors did not affect the measurements. The measurement of thermal contact resistance of all 30 samples on each measurement occasion required 3 working days. This measurement time has not been included in the lifetime calculation.

For two samples, also denoted in the sample names as the Advance Group (AG), one without film with sample name "ON0/DRef1AG", and one with 12.5 µm silver film with sample name "S6/n11AG", we started the accelerated test 10 weeks before all the other samples, with the purpose to give an indication of the experiment functionality and the behavior of thermal contact resistance. These two samples were tested 28 weeks, corresponding to 18.8 years operating lifetime.

2.7. Calculation Method of the Acceleration Factor

Failure rates (R) for temperature-dependent failure mechanisms can be described by the Arrhenius Equation (1).

$$R = A \times exp\,(-E_A/kT_1) \quad (1)$$

where R denotes the failure rate, E_A is the activation energy of the dominant, temperature-dependent failure mechanism, k is Boltzmann's constant k = 0.0000862 eV/K and T_1 is the typical average temperature of the device during its lifetime. A is a pre-exponential, material-dependent constant.

To accelerate temperature-dependent failures, an accelerated lifetime test must be carried out at a temperature (T_2) significantly higher than the average temperature during lifetime. The acceleration factor, AF, for the test is calculated with the help of two Arrhenius equations at T_1 and T_2, respectively; see Equation (2), comparing two cases: the operating life at a typical average case-to-heat sink interface temperature at T_1 = 55 °C in normal operation compared to the oven temperature of the accelerated test at T_2 = 110 °C in this investigation. This calculation method of the acceleration factor, AF, follows the JEDEC standard, given in the JEDEC publication 122H [19].

$$AF = exp\ ((E_A/k) \times ((1/T_1) - (1/T_2))) \quad (2)$$

This calculation formula is widely used in electronics technology and product qualifications. Since most failure modes in electronics, as well as failure models of interfaces due to migration or oxidation are significantly temperature dependent, the use of the Arrhenius equation is a valid and relevant method for investigations of thermal contact resistances. The activation energy describes how strong temperature dependence has a failure mechanism. A higher value of E_A means stronger temperature dependence and a larger acceleration factor. There are, however, many different failure modes in power electronics and at thermal interfaces such as migration, oxidation, etc. Even for the same failure mechanism, there are variations in activation energy depending on geometries, layer thicknesses and other environmental factors such as humidity. For example, the activation energy for corrosion can vary between 0.3 and 1.1 eV and for electromigration it can vary between 0.5 and 1.2 eV [20]. Since we do not know the exact failure mechanism in this study, we cannot precisely calculate the acceleration factor. We must rely on generally accepted empirical knowledge in electronic systems where a widely used value for activation energy is 0.7 eV. We use this value in our calculations, also, to get a comparable timeline to other accelerated test results in electronics. With this input data by using Equation (2), the calculation resulted in the acceleration factor of 35.0, assuming the component is in use 100% of time.

3. Results

3.1. Measurement Results at Start of the Accelerated Lifetime Test

The thermal contact resistance Rt was measured at the start of the lifetime test for all 30 samples. The results are summarized in Table 1 below.

Table 1. Measurement results of thermal contact resistance (Rt) of all 30 samples at start of the test in three groups: with no film, with 12.5 µm and 6 µm silver film.

No Film		**12.5 µm Silver Film**		**6 µm Silver Film**	
Sample Name	**Rt [K/W]**	**Sample Name**	**Rt [K/W]**	**Sample Name**	**Rt [K/W]**
N1/D7	1.47	OS21/2	1.15	S1t/4	1.58
N2/13	1.59	S2/6	1.67	S3t/8	1.68
N3/21	1.33	S4/10	1.53	S5t/11	1.74
N4/29	1.82	S6/n11AG	1.54	S7t/16	1.83
N5/D4	1.83	S8/18	1.23	S9t/20	1.5
ON6/48	2.74	S10/D6	1.56	S11t/24	1.48
ON0/DRef1AG	2.32	S12/26	1.49	S13t/28	1.73
		S14/D9	1.55	S15t/32	1.8
		S16/34	1.41	S17t/36	1.85
		S18/38	1.64	S19t/41	1.81
		S20/43	1.18	OS22t/45	1.9
		OS23/47	1.86		
Average	**1.87**	**Average**	**1.48**	**Average**	**1.72**
Min to Max	1.41	Min to Max	0.71	Min to Max	0.43
3 sigma no outliers	0.46	3 sigma no outliers	0.23	3 sigma no outliers	0.35
		% of No Film	**79.3**	**% of No Film**	**91.8**

The results show that on average the samples with silver film have lower thermal contact resistance compared to no-film samples. Specifically, 12.5 µm silver film samples have 79.3% and 6 µm samples have 91.8% of thermal contact resistance of no-film samples on average. Since the distribution of the measured thermal contact resistances are overlapping, we have made a statistical evaluation of the significance of these differences with unpaired t-tests. As expected, the difference of 20.7% between no film and 12.5 µm films is statistically significant, while the 8.2% difference between no-film samples and 6 µm film samples is statistically not significant.

Analysis of measurement results' distributions shows significantly higher difference between minimum to maximum (Min to Max) values for no-film samples (1.41 K/W) compared to 12.5 µm (0.71 K/W) and 6 µm (0.43 K/W) silver film samples. Taking out high outliers (above 1.85 K/W) and low outliers (below 1.30 K/W), the remaining samples show also higher 3 standard deviation (3 sigma) for no-film samples (0.46 K/W) compared to 12.5 µm (0.25 K/W) and 6 µm (0.35 K/W) silver film samples. This data supports a general observation of a significantly smaller variation of thermal contact resistances in samples using silver interlayer films.

3.2. Thermal Contact Resistance Behavior in the Beginning of Operating Lifetime

Significant changes have been observed in the thermal contact resistance during the first months of operating lifetime. Measurement results of all 30 samples show significant decrease in thermal contact resistance, on average 5%. This change happens both for samples without film and with silver films at both 12.5 µm and 6 µm thicknesses. Figure 5 below shows this initial behavior in four graphs.

Figure 5a shows the change on average of the different film groups: no film samples, 12.5 µm and 6 µm film samples. Figure 5b shows the behavior for each sample with no film, Figure 5c shows the 12.5 µm film samples, and Figure 5d shows the 6 µm film samples' behavior. For a better view, each of the four graphs starts with an insert with larger time scale for the first 0.2 year of operating life.

We can observe when comparing the graphs in Figure 5, that the average thermal contact resistance of no-film samples remains the highest during the first months of operating life compared to 6 µm and 12.5 µm film averages. The relative lower value of thermal contact resistance for 12.5 µm and 6 µm film samples compared to no-film samples remains unchanged during this time period.

Comparing the distribution of no-film samples in Figure 5b to 12.5 µm film samples in Figure 5c and 6 µm film samples in Figure 5d shows a much wider distribution for no-film samples compared to 12.5 µm samples and even tighter distribution for 6 µm samples. However, the average value of 6 µm samples is higher than the average of 12.5 µm samples.

The highest thermal contact resistance outlier is a no-film sample (heat sink No. 48.), with the roughest heat sink surface, the highest outlier among the 12.5 µm samples is a sample also with rough heat sink surface (heat sink No. 47.) and the highest outlier among the 6 µm samples is also a sample with rough heat sink surface (heat sink No. 45.). Those three heat sinks were also initially recognized to have significantly rougher surfaces than average. The relative difference in thermal contact resistance of these outliers compared to their group averages is highest among no-film samples and smallest among 6 µm samples.

3.3. Thermal Contact Resistance Behavior During 12.1 Years of Operating Lifetime

All 30 samples were submitted to continuing accelerated lifetime tests and the thermal contact resistances were measured after 1, 2, 4, 6, 8, 10, 12, 14, 16, and 18 weeks in the oven at 110 °C corresponding to a total of 12.1 years of operating lifetime. Figure 5 shows the thermal contact resistance behavior during 12.1 years of operating lifetime, in Figure 5a for sample group averages, Figure 5b for no-film samples, Figure 5c for 12.5 µm silver film samples and Figure 5d for 6 µm silver film samples.

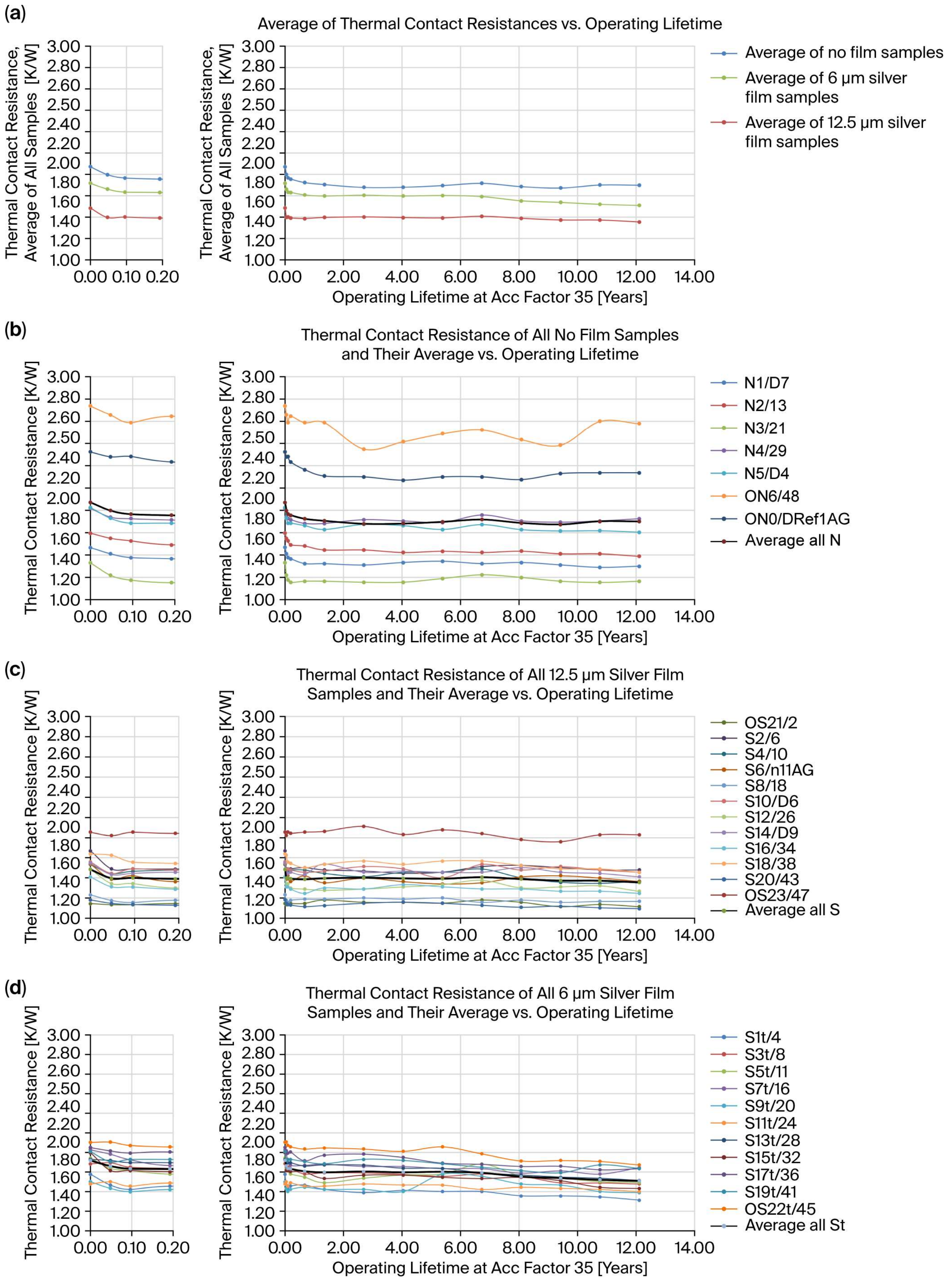

Figure 5. Thermal contact resistance behavior of 30 samples during 12.1 years of operating lifetime. (**a**) Film group averages of thermal contact resistance, (**b**) Thermal contact resistance for samples with no film and their average, (**c**) Thermal contact resistance for samples with 12.5 µm film and their average, (**d**) Thermal contact resistance for samples with 6 µm film and their average.

We observe that the average values of no-film, 12.5 µm and 6 µm silver film groups show a continuous, smooth behavior with no tendency of significant increase during the 12.1 years of operating lifetime, as shown in Figure 5a. Similarly to initial observations, the largest variation of thermal contact resistances is in the no-film group, significantly larger than that of the 12.5 µm and 6 µm silver film groups. The 6 µm silver film group has the smallest distribution, but their average value is higher than the 12.5 µm silver film group. As initially observed, we see that samples with the roughest heat sink surfaces continue to result in the highest thermal contact resistances, both in the group of no-film samples with heat sink No. 48, in the group with 12.5 µm silver film with heat sink No. 47, and also in the group of 6 µm silver film with heat sink No. 45. These rough surface samples show significantly larger measurement-to-measurement variations compared to their groups. In Figure 5d, we can see a small decreasing tendency of thermal contact resistances for the 6 µm silver film group, especially after 6 years.

In Table 2 below, we summarized thermal contact resistances of all 30 samples at the start of the test, at 12.1 years' operating lifetime, the averages and the percentages of changes.

Table 2. Summary of all 30 samples thermal contact resistances, Rt, at start and after 12.1 years of operating lifetime, the averages and the percentages compared start values and compared to no-film group.

No Film Samples Rt [K/W]				**12.5 µm Silver Film Samples Rt [K/W]**				**6 µm Silver Film Samples Rt [K/W]**			
Sample Name	**Rt at Start**	**Rt at 12.1 Years**	**% of Start**	**Sample Name**	**Rt at Start**	**Rt at 12.1 Years**	**% of Start**	**Sample Name**	**Rt at Start**	**Rt at 12.1 Years**	**% of Start**
N1/D7	1.47	1.3	88.5	OS21/2	1.15	1.12	97.3	S1t/4	1.58	1.31	83.2
N2/13	1.59	1.39	87	S2/6	1.67	1.48	88.7	S3t/8	1.68	1.48	87.8
N3/21	1.33	1.16	87.4	S4/10	1.53	1.37	89.5	S5t/11	1.74	1.49	85.5
N4/29	1.82	1.72	94.7	S6/n11AG	1.54	1.36	88.2	S7t/16	1.83	1.65	90
N5/D4	1.83	1.6	87.8	S8/18	1.23	1.17	94.8	S9t/20	1.5	1.39	92.6
ON6/48	2.74	2.58	94.2	S10/D6	1.56	1.46	93.3	S11t/24	1.48	1.4	94.7
ON0/DRef1AG	2.32	2.14	92	S12/26	1.49	1.27	85.2	S13t/28	1.73	1.51	87.5
				S14/D9	1.55	1.41	91.1	S15t/32	1.8	1.43	79.7
				S16/34	1.41	1.25	88.3	S17t/36	1.85	1.63	88.3
				S18/38	1.64	1.46	89	S19t/41	1.81	1.64	90.5
				S20/43	1.18	1.09	92.5	OS22t/45	1.9	1.67	87.8
				OS23/47	1.86	1.83	98.6				
Average	**1.87**	**1.7**	**90.2**	**Average**	**1.48**	**1.35**	**91.4**	**Average**	**1.72**	**1.51**	**88**
Min to Max	1.41	1.42	100.6	Min to Max	0.71	0.74	103.6	Min to Max	0.43	0.36	84.8
3 sigma no outlier	0.46	0.51	110.4	3 sigma no outlier	0.23	0.24	107.4	3 sigma no outlier	0.35	0.19	55.6
				% of No Film	**79.3**	**79.7**		**% of No Film**	**91.8**	**88.8**	

We can observe from the "% of start" columns in Table 2, that no samples' thermal contact resistance has reached its start value (100%). This presents the most important finding of this study, that no samples have failed, not even our outliers with the roughest heat sink surfaces. From the beginning of the test, we defined "failure" as 20% increase of the thermal contact resistance from its original value with the second limitation, that the power diode is not surpassing its maximum junction temperature rating before the 20% increase. Since we employed high maximum temperature diodes of 175 °C and ice water cooling of the heat sink, the maximum junction temperature limitation did not occur. Observing a general decrease in thermal contact resistance over the 12.1 years of lifetime, we did not need to employ our specific definition of failure.

We see a general decrease in thermal contact resistance after 12.1 years of operation of around 10%. Out of that 10%, around a 5% decrease occurs already during the first months of operation, as described earlier. Compared to the no film group, we see also after 12.1 years of operation lower thermal contact resistances on average of 20.3% for the 12.5 µm silver film group and of 11.19% for the 6 µm silver film group. Analysis of the distribution of thermal contact resistances between the start and 12.1 years of lifetime shows that the variation of thermal contact resistances slightly increases with a few percentages for the no-film group (100.6%) and the 12.5 µm silver film group (103.6%), while we see a decrease for 6 µm silver film group (84.8%). However, the variation of thermal contact resistances between samples in each group remains much smaller after 12.1 years lifetime for the 12.5 µm silver film group (min to max = 0.74 K/W) and the 6 µm silver film group (min to max = 0.36 K/W) compared the no-film group (min to max = 1.42 K/W). This supports a general observation of the advantage of using interlayer silver film to lower the variation in thermal contact resistance between samples. This observation remains valid also after 12.1 years of lifetime.

3.4. Thermal Contact Resistance Behavior of Advance Group Samples During 18.8 Years of Operating Lifetime

Two samples, called Advance Group as described in Section 2.6, started the 110 °C oven accelerated lifetime test 10 weeks earlier than all other samples, and therefore in total they had 28 weeks of oven time, corresponding to 18.8 years of operating lifetime. They were one sample with no silver film and one sample with 12.5 µm silver film. Figure 6 shows the results.

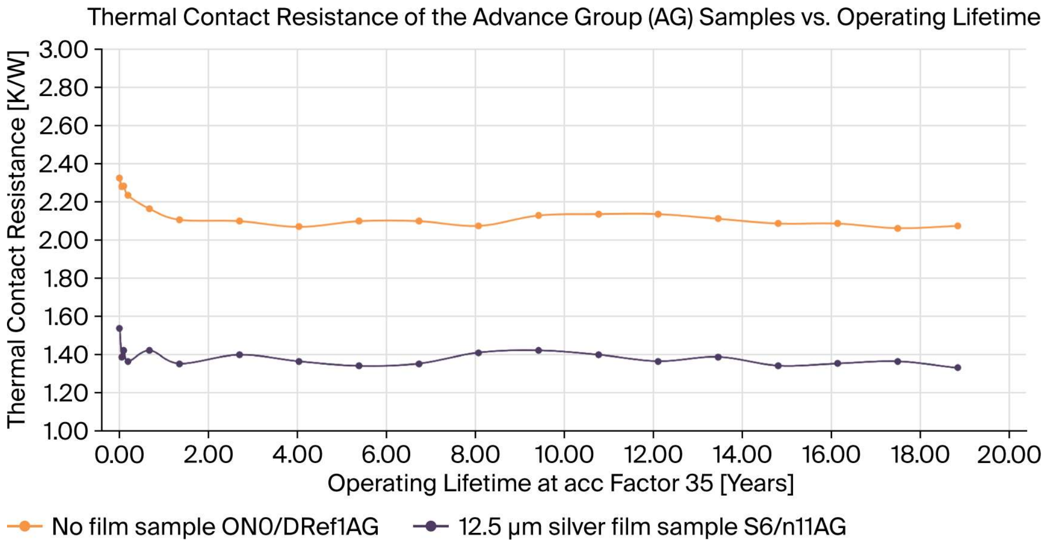

Figure 6. Two Advance Group samples' thermal contact resistances as a function of operating lifetime. "ON0/DRef1AG" sample without film and "S6/n11AG" sample with 12.5 µm silver film.

We can conclude from Figure 6 that no major changes in thermal contact resistance behavior occur between 12.1 and 18.8 years of operating life for these two samples, and the thermal contact resistance values are lower than at start of the lifetime test even after 18.8 years of operating lifetime.

3.5. Dissipated Power Dependence of Thermal Contact Resistance and Its Behavior During 12.1 Years of Operating Lifetime

Three samples have been analyzed for how their thermal contact resistance depends on dissipated power at the start of the lifetime test and at 4 years, 8 years and 12.1 years of lifetime. The first sample was named "N4/29" without film, the second sample was named "S12/26" with 12.5 µm silver film, and the third sample was named "S11t/24" with 6 µm silver film. The heat sinks' surfaces were nominal in these three samples. Figure 7 summarizes the results. Figure 7a shows the three sample thermal contact resistances at the start of the lifetime test and at 12.1 years of operating lifetime. Figure 7b shows the thermal contact resistance for the no-film sample (N4/29) at start, after 4 years, after 8 years and after 12.1 years of operating lifetime. Similarly, Figure 7c shows this data for the 12.5 µm silver film sample (S12/26) and Figure 7d does so for the 6 µm silver film sample.

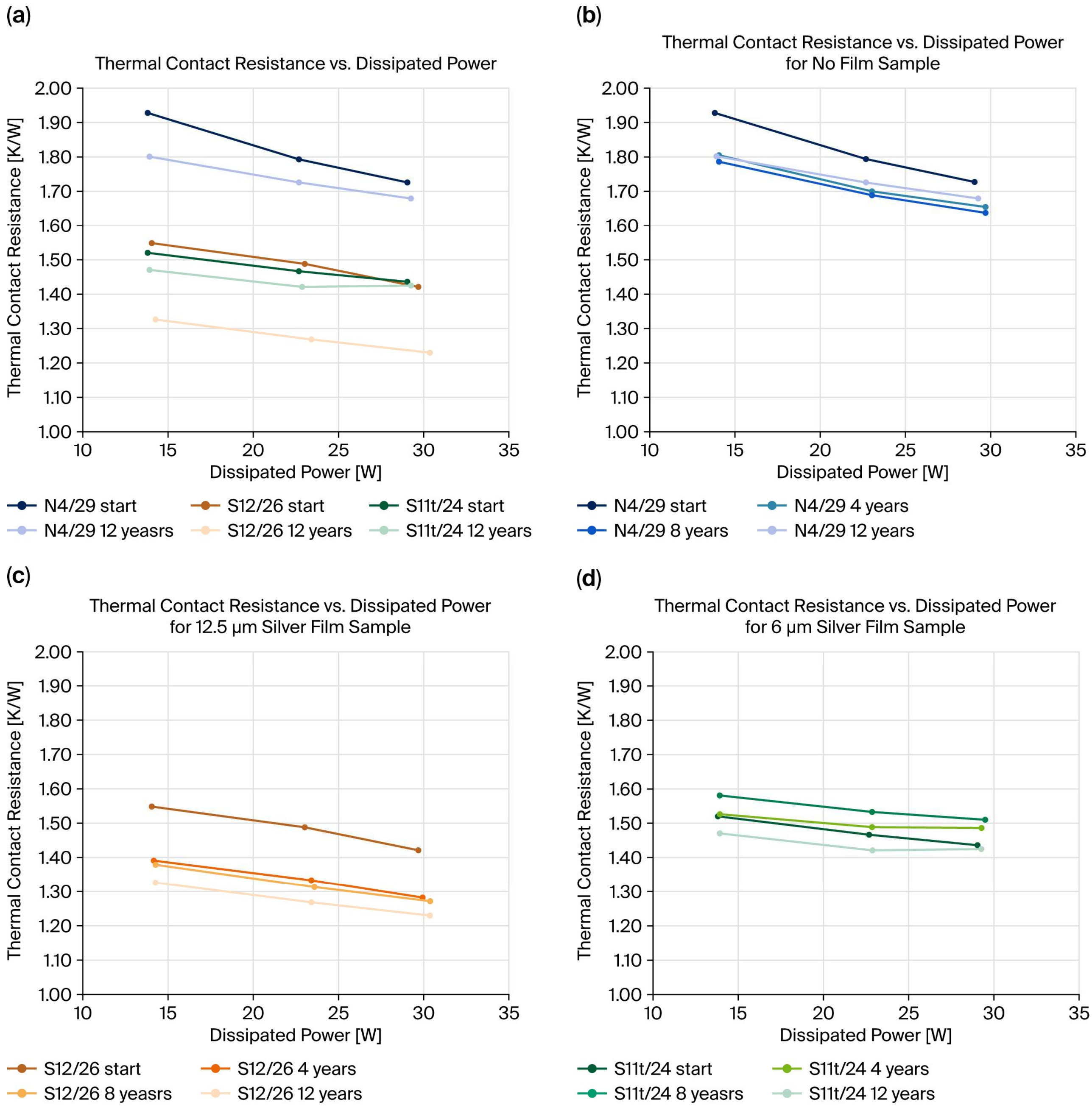

Figure 7. Thermal contact resistance vs. dissipated power of three samples during 12.1 years of operating lifetime. (**a**) Thermal contact resistance at start and after 12.1 years for 3 samples: No film, 12.5 µm, 6 µm film. (**b**) Thermal contact resistance of no-film sample at start and after 4, 8 and 12.1 years. (**c**) Thermal contact resistance of 12.5 µm film sample at start and after 4, 8 and 12.1 years. (**d**) Thermal contact resistance of 6 µm film sample at start and after 4, 8 and 12.1 years.

We observe from Figure 7 that all three samples show decreasing thermal contact resistance with increasing power dissipation, both at the beginning of the lifetime test and after 12.1 years of lifetime. This decreasing tendency is largest for the no-film sample and smallest for the 6 μm sample. The change in thermal contact resistance after the 12.1-year lifetime is largest for the 12.5 μm silver film sample and smallest for the 6 μm silver film sample. Because just a few samples were tested, none of the above observations are statistically proven.

3.6. Visual Comparative Surface Evaluation of Aged Silver Film Surface Compared to Unused Film

One sample with 12.5 μm silver film aged to 18.8 years of lifetime, named S6/n11AG from the Advance Group (AG), was opened after 28 weeks in the oven at 110 °C, and the silver film surface towards the heat sink was compared to an unaged silver film surface. A photograph of this comparison is shown in Figure 8.

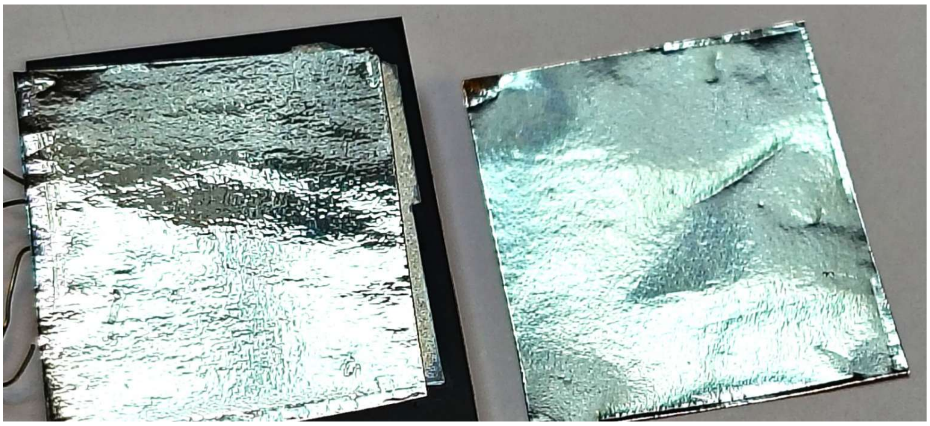

Figure 8. Visual comparison of a silver film surface after 18.8 years aging on the left side compared to an unused (unaged) silver film surface.

The sample with 12.5 μm silver film aged to 18.8 years of lifetime shows no significant discoloration due to oxidation compared to the unaged film. A small discoloration is present only on the left edge of the film. This points towards the conclusion that no significant in-diffusion of oxygen occurred during the aging process. We observe that the surface morphology has changed, as the surface becomes more rough and uneven for the aged silver film. This indicates that movement of the silver material could occur under aging and mechanical pressure.

4. Discussion

Results in Table 1 show that at the start of the lifetime test, samples with 12.5 μm silver film on average have 20.7% lower thermal contact resistances and samples with 6 μm silver film on average have 8.2% lower thermal contact resistances compared to the average of no-film samples. However, the thermal contact resistance distributions of these three groups are overlapping due to large variations of heat sink surface qualities, clip pressures and package thicknesses. Statistical analysis of the above differences shows that only the 12.5 μm thick silver film group's result of 20.7% lower average thermal contact resistance is statistically significant. Larger sample sizes of each group could have improved the statistical significance of the results. Analysis of distributions in Table 1 shows significantly smaller variations both for min to max and non-outlier samples' 3 sigma values for the silver film samples compared to no-film samples. These results indicate a mechanical interaction between the silver film and the heat sink and package surfaces. One hypothetical, not proven interaction is the softening of the silver film and consequently the silver filling out more microscopic voids between the TO 247 package and the heat sink. Therefore, the volume of air-filled voids diminishes, resulting in lower thermal contact resistance. Also, some co-planarity issues between the TO 247 package and the heat sink surfaces are possibly levelled out by silver films. This not-proven levelling out effect can be explained by the known Indentation Size Effect, where areas of silver film not in full contact with the package or heat sink due to non-planarity do not experience the full mechanical pressure, behaving harder and therefore remaining unchanged in thickness, while in areas experiencing the full mechanical pressure, the stress will result in more significant thinning of the film, pushing out silver material due to its high ductility. Published simulation results [8] show also optimization possibilities by thermal interface structures. For Press-pack type of packages, having much higher, ca. 20 MPa mechanical pressures, experimental results [21] also show an even larger, very significant decrease in thermal contact resistance due to the softening effect of the inserted ultra-thin silver film. In this investigation, the thermal contact resistance change is smaller due to much lower mechanical pressure from the clips, varying between 0.1 to 0.6 MPa.

We observed in Table 1 that the highest outliers in each group were the samples with the roughest heat sink surfaces, numbered 48, 47 and 45, respectively. This points out that the heat sink surface quality is a major parameter affecting thermal contact resistance. As Figure 3 demonstrates, a simple visual inspection of heat sinks' top surfaces could be a sufficient method to exclude these outliers. The thermal contact resistance improvement on average is more than double for the 12.5 μm film group than for the 6 μm group, indicating that other factors than only the silver material softening are responsible for the improvement compared the no-film group. As previously known, silver has a high ductility, manifested in the high Poisson Ratio of 0.3, representing that the perpendicular strain of silver is 30% of the strain in the direction of stress. At the same clip pressure, this results in double elongation of 12.5 μm film compared to 6 μm silver film; consequently, the 12.5 μm can fill out more of the microscopic voids. In this study, we cannot unambiguously prove that this effect is the main responsible mechanism.

Figure 5 shows the thermal contact resistances of all samples and group averages during the operational life of 12.1 years. All samples and group averages exhibit a decrease of around 5% in thermal contact resistances in the first operational month. We can attribute this effect to the possible softening of sharp top edges of the heat sink contact surfaces [22]. This decrease is not dependent if we use a thermal interface material but contributes positively to the thermal contact resistance stability. If we compare the thermal contact resistance distributions in Figure 5b with Figure 5c,d, we see smaller variations within the 12.5 μm and the 6 μm groups, compared the no-film group. This shows that the smaller variations within the silver film groups remain also during the operating lifetime. This is an additional advantage of using ultra-thin silver interface films.

An important result of this study is shown in Table 2. None of the 30 samples fail after the accelerated lifetime test corresponding to 12.1 years of lifetime. This indicates that there is no inherent failure mode between a clip-attached TO 247 package and aluminum heat sink in an indoor, steady state environment, which should limit the lifetime below 12.1 years. This important result is, however, limited to indoor, dc type of applications, since no power cycling [23], humidity, nor vibration or mechanical shock test were included in this study [24].

We see that thermal contact resistances are improving and getting lower in an accelerated lifetime test even as long as 18.8 years lifetime for a few samples evaluated, as shown in Figure 6. Several previously known stabilizing mechanisms can give hypothetical explanations for this improvement. Firstly, the sharp tops of the aluminum heat sink surface are smoothing out due to the applied mechanical pressure already at the beginning of the operating life affecting all samples. Secondly, the high ductility manifested in a high Poisson Ratio of 0.3 of silver makes inserted silver films better at filling out microscopic voids. This effect is larger for the 12.5 μm silver film than for the 6 μm silver film. Thirdly, the stress-strain characteristics for silver [25] show a large temperature dependency where already at 50 °C to 60 °C some early plasticity occurs. This effect is fully reversible when temperature goes down. The Indentation Size Effect [26,27] can also contribute to the observed smaller thermal contact resistance improvement with 6 µm film than 12.5 µm film. Finally, also the softness [28] of the silver material is contributing to level out surface non-planarity. We have been able to observe changes in the surface structure indicating a possible movement of silver material in aged films compared to non-aged films in Figure 8 but not able to directly point out and prove which of the above known stabilizing mechanisms are responsible for the lower thermal contact resistance. Further analysis of the aged film compared to new film would be needed to identify the responsible mechanism. Such analysis could be SEM/EDS or 3D surface measurements [29]. Among the above-mentioned stabilizing mechanisms, we think that the material softening and the high ductility mechanisms are the most plausible explanations. To evaluate this hypothesis and distinguish between different mechanisms, we propose to evaluate other materials such as aluminum films, since aluminum is a harder material but has a similar, high ductility as silver. Possibly several of these physical effects contribute to lowering the thermal contact resistance [30] over the operating lifetime.

The clip-induced mechanical pressure is also one important affecting parameter for changes in thermal contact resistance. It does not seem to degrade during the lifetime of 12.1 years.

One known phenomenon that could increase thermal contact resistance is oxidation of interface surfaces in vicinity of the microscopic voids that can produce high thermal resistance oxides. This phenomenon does not seem to occur in this study done in an indoor environment and not at enhanced humidity.

An additional stabilizing result is presented in Figure 7. The thermal contact resistance is getting lower with increasing dissipated power and consequently with higher TO 247 contact surface temperature, regardless of the use of interlayer silver films. One probable explanation is that when the TO 247 package gets warmer, it expands also in thickness, and therefore increases the mechanical pressure from the clip, resulting in smaller microscopic voids. This phenomenon will also have a stabilizing effect.

In the search for other, less expensive thermal interface material, ultra-thin aluminum film with high ductility and Poisson Ratio is an interesting candidate. The cost of ultra-thin high-purity aluminum films is approximately 30% of silver films or less.

5. Conclusions

1. The main novelty of this study is the detailed measurement results during the operating lifetime of the thermal contact resistance between a clip-attached TO 247 package and aluminum heat sink. We evaluated 30 samples with and without thin interlayer silver films by an accelerated lifetime test.

2. The main finding is that no failures in thermal contact resistances occurred in 30 samples after 18 weeks of accelerated lifetime test at 110 °C with the calculated acceleration factor of 35, corresponding to 12.1 years of operating lifetime in an indoor environment. Not even samples with high, outlier thermal contact resistances failed. All samples show improved, lowered thermal contact resistances on average of 10% after 12.1 years of lifetime. From this 10%, an initial lowering of 5% occurs during the first months of operating life. Two samples, one with 12.5 µm silver film, one with no film have been evaluated even for a longer operating lifetime of 18.8 years, where no failures, nor significant changes in thermal contact resistance, have been observed. We observed silver material surface changes indicating material movement could occur in aged silver films, but no single mechanism could be pointed out and proven to be responsible for the lowered thermal contact resistances.

https://doi.org/10.3390/en19153493

We can, however, conclude that stabilizing aging mechanisms are dominant during this indoor environmental lifetime test.

3. Samples with 12.5 μm silver film show on average 20% lower thermal contact resistance than the average of no-film samples. Samples with 6 μm silver film show on average 8% to 11% lower thermal contact resistance than the average of no-film samples. Samples with 12.5 μm and 6 μm silver films show smaller variations of thermal contact resistance than no-film samples. From these results, we can conclude that there is an advantage in using ultra-thin silver films as thermal interface material.

4. We could identify high outlier thermal contact resistances for samples with very rough heat sink contact surfaces. We conclude that it is possible to prevent high outlier thermal contact resistances by a visual inspection of heat sink contact surfaces.

5. We demonstrated that increased power dissipation, with higher package temperature, results in lower thermal contact resistance. This has also a stabilizing effect.

Supplementary Materials: The following supporting information can be downloaded at: https://www.mdpi.com/article/10.3390/en19153493/s1.

Author Contributions: Conceptualization, Z.T.-P. and H.-P.N.; Methodology, Z.T.-P. and H.-P.N.; Formal analysis, Z.T.-P.; Investigation, Z.T.-P.; Resources, H.-P.N.; Data curation, Z.T.-P.; Writing—original draft, Z.T.-P.; Writing—review and editing, Z.T.-P. and H.-P.N.; Supervision, H.-P.N.; Funding acquisition, H.-P.N. All authors have read and agreed to the published version of the manuscript.

Funding: This research received no external funding.

Data Availability Statement: The original contributions presented in this study are included in the article/Supplementary Materials. Further inquiries can be directed to the corresponding author.

Conflicts of Interest: The authors declare no conflict of interest.

References

1. Italia, R. An Analysis of Heat dissipation techniques in power Electronics. *J. Eng. App. Sci. Technol.* **2023**, *5*, 1–6. [CrossRef]
2. Orville, T.; Tajwar, M.; Bihani, R.; Saha, P.; Hannan, M.A. Enhancing Thermal Efficiency in Power Electronics: A Review of Advanced Materials and Cooling Methods. *Thermo* **2025**, *5*, 30. [CrossRef]
3. Rahman, I.; Moghassemi, A.; Arsalan, A.; Timilsina, L.; Chamarthi, P.K.; Papari, B.; Ozkan, G.; Edrington, C.S. Emerging trends and challenges in thermal management of power electronic converters: A state of the art review. *IEEE Access* **2024**, *12*, 50633–50672. [CrossRef]
4. Li, Y.; Roux, S.; Castelain, C.; Fan, Y.; Luo, L. Design and Optimization of Heat Sinks for the Liquid Cooling of Electronics with Multiple Heat Sources: A Literature Review. *Energies* **2023**, *16*, 7468. [CrossRef]
5. Morel, C.; Morel, J.-Y. Power Semiconductor Junction Temperature and Lifetime Estimations: A Review. *Energies* **2024**, *17*, 4589. [CrossRef]
6. Zhou, Y.; Wu, S.; Long, Y.; Zhu, F.; Liu, F.; Murugadoss, V.; Winchester, W.; Nautial, A.; Wang, Z.; Guo, Z. Recent advances in thermal interface materials. *ES Mater. Manuf.* **2020**, *7*, 4–24.
7. Stoyek, K.; Nowak, A.-K.; Rac-Rumijowska, O. Ag microparticle/Au nanoparticle thermal interface materials sintered at low temperatures and pressure. *Materials* **2025**, *18*, 4981. [CrossRef] [PubMed]
8. Singhal, V.; Siegmund, T.; Garimella, S. Optimization of Thermal Interface Materials for Electronics Cooling Applications. *IEEE Trans. Compon. Packag. Manuf. Technol.* **2004**, *27*, 244–252. [CrossRef]
9. Wei, B.; Luo, W.; Du, J. Thermal interface materials: From fundamental research to applications. *Susmat* **2024**, *4*, 239. [CrossRef]
10. Jagt, J.C. Reliability of Electrically Conductive Adhesive Joints for Surface Mount Applications: A Summary of the State of the art. *IEEE Packag. Manuf. Technol. Part A* **1998**, *21*, 215–225. [CrossRef]
11. Wang, L.; Rietveld, G.; Hueting, R.-J.-E. Thermal shock reliability of silver-sintered bonding of metal-plated aluminum surfaces. *IEEE Trans. Device Mater. Reliab* **2025**, *25*, 203–211. [CrossRef]
12. Muzychka, Y.; Yovanovich, M. Chapter 10 Introduction to Thermal Contact Resistance. In *Thermal Spreading and Contact Resistance: Fundamentals and Applications*, 1st ed.; John Wiley & Sons, Inc.: Newark, NJ, USA, 2023.
13. Yovanovich, M.; Culham, J.R.; Teerstra, P. Calculating interface resistance. *Electron. Cool.* **1997**, *3*, 21–29.

14. Toth-Pal, Z.; Nee, H.-P. Thermal Contact Resistance Improvement Between Clip Attached TO-247 Package and Heat Sink with Insertion of an Ultra-Thin Interlayer Silver Film. In Proceedings of the 2025 31st International Workshop on Thermal Investigations of ICs and Systems (THERMINIC), Naples, Italy, 24–26 September 2025; pp. 1–4. [CrossRef]
15. Poppe, A.; Szekely, V. Dynamic Temperature Measurements: Tools Providing a Look into Packaging and Mount Structures. *Electron. Cool.* **2002**, *8*, 10–19.
16. Bosch, E.G.T. Accurate Measurement of Interface Thermal Resistance by Means of a Transient Method. In Proceedings of the 16th Annual IEEE Semiconductor Thermal Measurement and Management Symposium, San Jose, CA, USA, 23–23 March 2000; pp. 167–173.
17. ONSEMI. Application Note, Power Packages Heat Sink Mounting Guide. May 2022, Rev 3. Publication Order No.: AND9859/D. Available online: https://www.onsemi.com (accessed on 21 July 2026).
18. Tulkoff, C.; Caswell, G. Chapter 2 Establishing a reliability program. In *Design for Excellence in Electronics Manufacturing*; Wiley: Hoboken, NJ, USA, 2021.
19. JEDEC Publication 122H. pp. 2–3. Available online: https://standards.globalspec.com/std/10047309/jedec-jep-122 (accessed on 21 July 2026).
20. Basha, M.; Ware, N.R. Design validation and reliability of electronic systems using next generation RGT models. *Def. Sci. J.* **2023**, *73*, 594–601. [CrossRef]
21. Toth-Pal, Z.; Zhang, Y.; Below, I.; Nee, H.-P.; Bakowski, M. Investigation of Pressure Dependent Thermal Contact Resistance between Silver Metallized SiC Chip and DBC Substrate. *Mater. Sci. Forum* **2015**, *821-823*, 452–455. [CrossRef]
22. Quin, F.; Zhao, S.h.; Yanwei, D.; Liu, L.; An, T.; Chen, P.; Gong, Y. Indentation tests of sintered silver in Die-attach interconnection after thermal cycling. *J. Electron. Packag.* **2022**, *144*, 031012.
23. Paret, P.; Major, J.; DeVoto, D.; Narumanchi, S.; Ding, C.h.; Lu, G.-Q. Reliability and lifetime prediction model of sintered silver under high-temperature cycling. *IEEE J. Emerg. Sel. Top. Power Electron.* **2021**, *10*, 5181–5191. [CrossRef]
24. Due, J.; Robinson, A.J. Reliability of thermal interface materials: A review. *Appl. Therm. Eng.* **2013**, *50*, 455–463. [CrossRef]
25. Wakamoto, K.; Mochizuki, Y.; Otsuka, T.; Nakahara, K.; Namazu, T. Temperature dependence on tensile machanical properties of sintered silver film. *Materials* **2020**, *13*, 4061. [CrossRef] [PubMed]
26. Shen, Z.; Su, Y.; Liang, Z.; Long, X. Review of indentation size effect in crystalline materials: Progress, challenges and opportunities. *J. Mater. Res. Technol.* **2024**, *31*, 117–132. [CrossRef]
27. Bull, S.-J. On the origins and mechanisms of the indentation size effect. *Z. Für Met.* **2003**, *94*, 787–792. [CrossRef]
28. Gökdeniz, Z. Reliability of Silver Sintered Large Area Joints: Temperature Dependent Properties Under Static and Cyclic Loading. Ph.D. Dissertation, Faculty of Technical Chemistry, TU Wienna, Vienna, Austria, 2022.
29. Chen, L.; Li, S.; Zhu, S.; Wang, T.; Huang, Q.-X. Physicochemical co-evolution of SUS304 ultra-thin steel foils induced by laser and its effect on interface bonding of steel/CFRP joints. *J. Iron Steel Res. Int.* **2026**, *33*, 80. [CrossRef]
30. Tatsumi, H.; Kumada, S.h.; Fukada, A.; Yamaguchi, H.; Kashiba, Y. Impact of metallurgical and mechanical properties of sintered silver joints on die-attach reliability of high-temperature power modules. *J. Microelectron. Electron. Packag.* **2016**, *13*, 121–127. [CrossRef]